Photochemical & Photobiological Sciences

PAPER

Cite this: *Photochem. Photobiol. Sci.*, 2016, **15**, 1124

New insight into the photophysics and reactivity of trigonal and tetrahedral arylboron compounds†

Willy G. Santos,*[a] João Pina,[b] Douglas H. Burrows,[b] Malcolm D. E. Forbes*[c] and Daniel R. Cardoso[a]

Received 30th May 2016,
Accepted 5th August 2016

DOI: 10.1039/c6pp00169f

www.rsc.org/pps

The photophysics and reactivity of two tetraphenylborate salts and triphenylborane have been studied using ultrafast transient absorption, steady-state fluorescence, electron paramagnetic resonance with spin trapping, and DFT calculations. The singlet excited state of tetraarylborates exhibit extended π-orbital coupling between two adjacent aryl groups. The maximum fluorescence band, as well as the transient absorption bands centered at 560 nm (τ = 1.05 ns) and 680 nm (τ = 4.35 ns) are influenced by solvent viscosity and polarity, indicative of a twisted intramolecular charge transfer (TICT) state. Orbital contour plots of the HOMO and LUMO orbitals of the tetraarylboron compounds support the existence of electron delocalization between two aryl groups in the LUMO. This TICT-state and aryl–aryl electron extension is not observed for the trigonal arylboron compound, in which excited π-orbital coupling only occurs between the boron atom and one aryl group, which restricts the twist motion of the aryl–boron bond. The excited triplet state is deactivated primarily through aryl–boron bond cleavage, yielding aryl and diphenylboryl radicals. In the presence of oxygen, this photochemistry results in phenoxyl and diphenylboroxyl radicals, as confirmed by EPR spectroscopy of spin trapped radical adducts. The TICT transition and radical generation is not expected for BoDIPY molecules where the rotational vibration of the B–aryl bond is rigid, restricting changes in the geometric structure. In this sense, this work contributes to the development of new BoDIPY derivatives where the TICT transition may be observed for aryl ligands with free rotational vibrations in the BoDIPY structure.

Introduction

The photophysics and photochemistry of arylboron compounds are an important but relatively underinvestigated subfield of nonlinear optics (NLO). The unusual behavior of the excited states of organoboron compounds has provided new avenues of exploration for improving the photonic properties of hybrid materials.[1–11] In particular, these compounds combine the properties of extended organic π-systems with the unique features of semi-metals, leading to novel materials with many desirable chemical and physical properties (larger extinction coefficients, Lewis acid–base reactivity, stronger emission intensities, *etc.*).[4,12–20]

The presence of the empty p_z orbital on the trigonal boron atom and its effective π-electron extension with attached aryl groups has been used to advantage by several research groups to provide new candidates for modern optoelectronic materials.[5–7,12] The replacement of selected carbon atoms with main-group heteroatoms such as boron has proven useful in circumventing some shortcomings of purely organic systems.[1,2,8,21–24] Such strategies can provide a powerful alternative to carbon-based photochemistry and photophysics by allowing access to novel electronically excited states. For example, the Lewis acidic character of boron atoms has led to interesting chemical, spectroscopic and optoelectronic properties, such as the intense luminescence found in certain semiconductor materials.[1,5,6,21,25] This effect is rooted in the interaction of the vacant p_z orbital at the boron center with the surrounding π-electron clouds in the trigonal molecule, which generally lowers the energy of molecule's lowest-unoccupied molecular orbitals (LUMO).

Gieseking and co-workers[9] reported excited-state and NLO properties of tetraphenylborate, describing the geometric and electronic structures of these molecules, which present three dimensional π systems that do not correspond with the geometric parameters typically used to understand linear

[a]*Instituto de Química de São Carlos, Universidade de São Paulo, São Carlos, SP, 13560-390, Brazil. E-mail: willy_glen@yahoo.com.br*
[b]*Universidade de Coimbra, Departamento de Química, Centro de Química, 3004-535 Coimbra, Portugal*
[c]*Center for Photochemical Sciences, Department of Chemistry, Bowling Green State University, Bowling Green, OH 43403, USA. E-mail: forbesm@bgsu.edu*

†Electronic supplementary information (ESI) available: DFT calculations results with chemical structure and $x:y:z$ coordinates, light scattering, UV-vis absorption and ultrasfast transient absorption spectra. See DOI: 10.1039/c6pp00169f

conjugated systems. However, quantitative spectroscopic information on these systems is limited. In particular, the differences in photophysical processes and photochemical reactions between trigonal and tetrahedral arylboron compounds have not been thoroughly explored.

Trivalent boron species typically have Lewis acid characteristics, while for tetrahedral compounds the boron atom behaves as Lewis base. Thus, the interaction between the p-orbitals of neighboring aryl groups bonded to a central boron atom is expected to be different for the two structures.

Several previous reports regarding the photochemistry of trigonal and tetrahedral arylboron compounds have detailed the photoproducts of the reactions, but very few have provided experimental measurements related to the excited-states and/or transition states involved.[26–36]

It is possible that an intramolecular charge transfer (ICT) process between the central boron atom and attached aryl groups may explain this difference, as observed for several organic and hybrid molecules.[37–44] The existence of twisted intramolecular charge transfer (TICT) and localized excited (LE) states is usually proposed to rationalize the dual emission observed in arylboron compounds and some other organic molecules.[24,45–52] The presence of a charge transfer state (CT-state) has not been confirmed or refuted for arylboron compounds, and to date there are few reports on the excited state dynamics of any trigonal and tetrahedral arylboron species. Motivated by this situation, this paper explores the excited-state dynamics and reaction mechanisms of several photoexcited organoboranes in greater detail, using electron paramagnetic resonance (EPR), and time resolved and steady state UV-VIS absorption and fluorescence spectroscopies. These are complemented by DFT calculations on the singlet and triplet states.

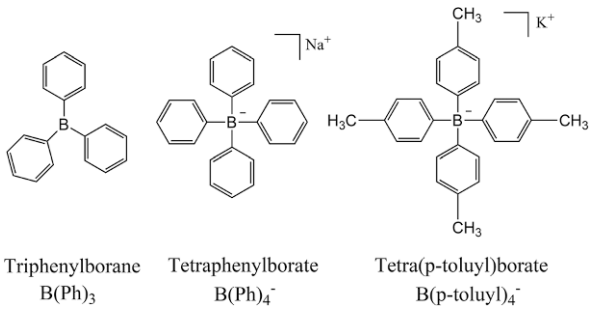

Scheme 1 Chemical structures and abbreviations of the arylboron compounds studied in this work.

Experimental

Materials

5,5-Dimethyl-1-pyrroline *N*-oxide 97.0% (DMPO), 2-aminoethyldiphenylborane 98.9% (2-APB), dimesitylboronic acid 99.0% (DMBA), phenylboronic acid (PhBOH), triphenylborane in THF (0.25 mol L^{-1}) 98.9% $B(Ph)_3$, tetraphenylboroxane (TPhB) 98.0%, sodium tetraphenylborate 99.5% ($Na^+B(Ph)_4^-$) and sodium tetra(*p*-toluyl)borate 99.0% ($Na^+B(p\text{-toluyl})_4^-$) were purchased from Sigma-Aldrich (Steinheim, Germany) and used without further purification. Solvents: acetonitrile (ACN), ethanol (EtOH), ethylene glycol (ETG), hexanol (HexOH), methanol (MetOH), propanol (PrOH), were of HPLC grade and purchased from Sigma-Aldrich (Steinheim, Germany). Anaerobic conditions were achieved by purging samples with high-purity argon (White-Martins, Sertãozinho-SP, Brazil) for 15–30 min prior to measurement. Stock solutions of arylboron compounds (10^{-2} mol L^{-1}) were freshly prepared using the appropriate solvent and stored in the dark at 278 K before all experiments. Scheme 1 shows the major arylboron compounds studied in this work.

Steady-state absorption and luminescence

UV-VIS absorption spectra were recorded using a Multskan Go Reader (Thermo Scientific, Waltham MA, US) or a Shimadzu UV 3600 (Hitachi-Hitech, Tokyo, Japan) spectrophotometer. Fluorescence spectra were recorded using a Hitachi F4500 (Hitachi-Hitech, Tokyo, Japan) spectrophotometer. Fluorescence and phosphorescence (77 K) quantum yields were measured using naphthalene as a standard (Φ_F = 0.21 and Φ_P = 0.05 in ethanol).[53,54]

The energy of the singlet state, E_S, was determined from the crossing point of the normalized excitation and fluorescence emission spectra of the investigated compounds. The energy of the lowest triplet state, E_T, was determined from the lowest vibronic band maximum observed in the phosphorescence spectra or from the shortest wavelength values observed in the phosphorescence spectra of the compound (the latter values were used only in the case where no vibronic structure was observed).

Laser flash photolysis

Transient difference absorption spectra were obtained using a laser flash photolysis instrument (Applied Photophysics Ltd, Surrey, United Kingdom) pumped by the fourth harmonic of a nanosecond Nd:YAG laser (Spectra Physics, Stahnsdorf, Germany) with excitation wavelength at 266 nm. First-order decay kinetics were observed for the lowest triplet state. Transient absorption spectra (300–650 nm) were recorded by monitoring the optical density change at 5 nm intervals, signal averaging at least 8 decays at each wavelength.

Electron paramagnetic resonance (EPR) spectroscopy

X-band (9.5 GHz) EPR measurements were carried out at 298 K using a TE_{102} rectangular cavity with 100 kHz magnetic field modulation and 1 G modulation amplitude (EMX plus, Bruker BioSpin, Rheinstetten, Germany). Organoborane solutions (10^{-3} mol L^{-1}) were prepared with addition of 100 mM of the spin trap, DMPO, in ethanol. Light irradiation of the boron compound was carried out using a 200 W mercury lamp (1800 mW m^{-2} nm^{-1}/200–300 nm spectral range) placed at 0.5 m from the cavity optical window. Measurements were performed in the absence of oxygen at different irradiation times.

Arylboron radical species were detected at 77 K in the absence of spin-trap, the concentration of the organoboranes were 10^{-2} mol L^{-1} and light irradiation performed in a 2 mm i.d. EPR Suprasil quartz tube (Sigma-Aldrich, Steinheim, Germany).

Ultrafast femtosecond transient absorption

Ultrafast spectroscopic and kinetic measurements were carried out using a broadband (350–1600 nm) HELIOS pump–probe femtosecond transient absorption spectrometer (Ultrafast Systems, Florida, United States), equipped with an amplified femtosecond Spectra-Physics Solstice-100F laser (displaying a pulse width of 128 fs with a 1 KHz repetition rate) coupled with a Spectra-Physics TOPAS Prime F optical parametric amplifier (195–2200 nm) for pulse pump generation. Probe light in the UV range was generated by passing a small portion of the 795 nm light from the Solstice-100F laser through a computerized optical delay (time window = 8 ns) and focusing in a vertical translating CaF_2 crystal to generate continuum white-light (350–750 nm). All measurements were carried out using 2 mm quartz cuvette with sample absorptions in the range of 1.0–1.8 at the pump light excitation wavelength. To avoid sample photodegradation, sample solutions were continuously stirred during the experiments and the irradiation area changed using a motorized translating sample holder. Transient absorption data were analyzed using the Surface Xplorer PRO proprietary software from Ultrafast Systems.

Theoretical calculations

Density functional theory (DFT) calculations were performed with the Gaussian 09 (G09) program package, employing the functional B3LYP. The basis set 6-31+(d,p) was used to optimize the gas phase singlet and triplet geometries with SCF-tight convergence criteria. All calculations resulted in positive vibrational frequencies.

Results and discussion

Steady-state photophysics

The UV/VIS absorption spectra of $B(Ph)_4^-$ and $B(p\text{-toluyl})_4^-$ (Scheme 1 for structures, Fig. S1 for absorption (ESI†) and Fig. 1 for excitation spectra) in ethanol display two intense, structureless bands in the near ultraviolet region.

For $B(Ph)_4^-$ the absorption bands are centered at 230 nm (ε_{max} = 11 500 mol^{-1} L cm^{-1}), and 265 nm (ε_{max} = 2200 mol^{-1} L cm^{-1}). For $B(p\text{-toluyl})_4^-$ the absorption bands were centered at 230 nm (ε_{max} = 30 000 mol^{-1} L cm^{-1}) and at 280 nm (ε_{max} = 4800 mol^{-1} L cm^{-1}) and for the $B(Ph)_3$ molecule, the UV/VIS spectrum shows two well defined absorption bands around 240 nm (ε_{max} = 4000 mol^{-1} L cm^{-1}) and 270 nm (ε_{max} = 3000 mol^{-1} L cm^{-1}).

As previously reported for benzene and $B(Ph)_4^-$,[5,21,22,53–57] the electronic absorption bands are characteristic of π–π* transitions from the aryl-group to the π-extended orbitals around the arylboron sites. As with benzene, the more intense band at shorter wavelengths is assigned to the E-band ($S_0 \rightarrow S_2$), which originates from an allowed transition, whereas the low intensity band at longer wavelength arises from the forbidden K-band ($S_0 \rightarrow S_1$) transition. This band exhibits three vibronic features, as shown in Fig. S1 (ESI†).

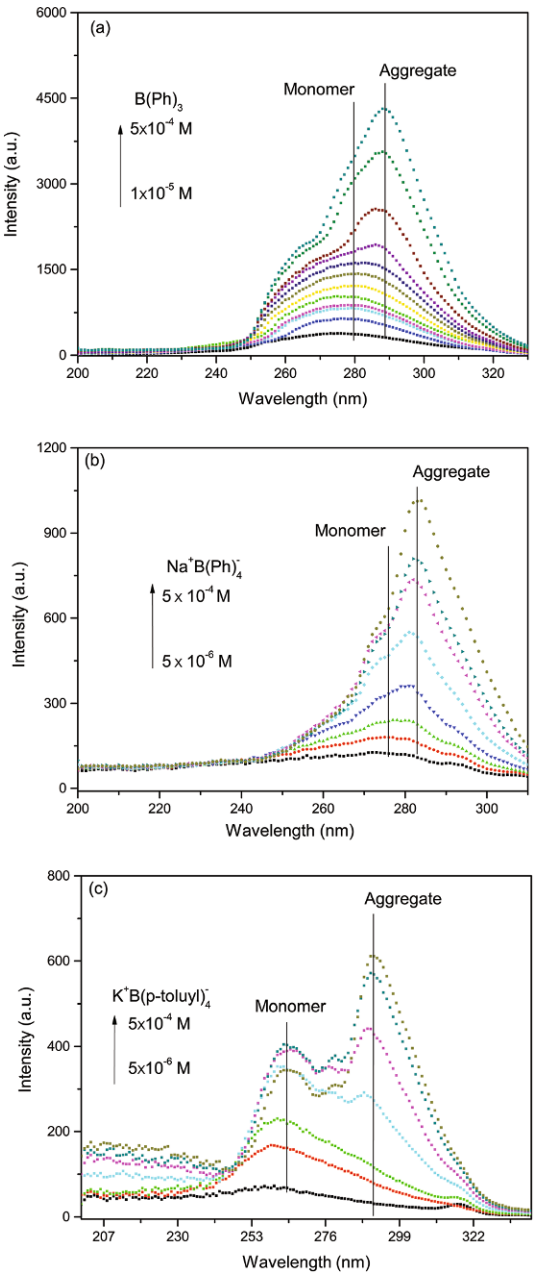

Fig. 1 Excitation spectra of (a) $B(Ph)_3$, (b) $B(PH)_4^-$ and (c) $B(p\text{-toluyl})_4^-$ recorded at different concentrations in ethanol at 298 K, λ_{em} = 340 nm.

For all three compounds, no appreciable change in the λ_{max} of the electronic absorption bands was observed in different polarity solvents. However, the maximum of the fluorescence emission band was shifted for all compounds. Matsumi and co-workers have reported similar results for *para*-substituted arylboron compounds.[58] This shift of the emission maximum is due to the high dipole moment of the excited state.

For all three structures, the lack of changes in the absorption band with solvent can be attributed to the similar polarity of the ground-states and vertically excited states, as demonstrated by the proximity of the dipole moment in our DFT calculation results, *vide infra*. In the ground and excited states, the molecular symmetry of the tetrahedral geometries implies that the dipole moment $\mu_g = 0$, as calculated for the ground-state. In the singlet excited state (in the absence of any charge transfer processes), the π*-orbitals are symmetrically distributed in the tetrahedral structure. A single excitation between these orbitals does not change the overall molecular dipole moment. However, if the excited states only involve transitions among non-degenerate orbitals, all excitations may have null contributions to μ_e and consequently $\Delta\mu_{ge}$ is zero.

If the contributions from excited states are different for the phenyl-boron* (locally excited state or LE) and for the CT state (or intramolecular charge transfer – ICT), as observed in trigonal and tetrahedral arylboron compounds, then their overall contribution to that state's dipole moment will be non-zero. In this case, the excited CT-state deactivation will be modulated by solvent polarity and ionic effects, with appreciable differences in the fluorescence emission spectra and fluorescence quantum yield.

T. Alaviuhkola and co-workers[60] reported the significant influence of the cation in the tetraarylborate structure, where the potassium cation and the tetraarylborate anions form a complex. In this case, each potassium cation is packed between two hosts with strong cation–π interactions. Ion pairing has a significant contribution of face-to face π···π and edge to face H···π contacts of phenyl rings, which may induce changes in the tetraarylborate geometry. An interesting sequence of anion···cation···anion···cation··· is also observed in the crystal structure with a significant contribution of π···π interaction with the phenyl rings, such as those observed in J-aggregates of BoDIPY molecules.[61] Fig. 2a and b show, respectively, the effect of the solvent polarity and viscosity in the fluorescence spectra of $B(Ph)_4^-$. The emission and excitation spectra (Fig. 2) are not significantly altered at low concentrations of the BPh_4^-, ranging from 10^{-6} to 10^{-5} mol L^{-1}, indicating that aggregate formation is not observed under these conditions, and all spectral changes may be attributed to solvent effects.

A significant dependence of the fluorescence spectrum on the dielectric constant of the solvent is in agreement with the presence of an ICT and/or TICT evolved state from excited-state bond-order reversal and solvent reorganization in polar media. However, a decrease in fluorescence intensity with increasing solvent polarity suggests a solvent interaction (n- or π-interaction) with tetraarylbroates. Noticeably, and only for tetraarylborates, the fluorescence emission maximum is red shifted by 13 nm or more in polar solvents (ethanol, methanol and acetonitrile) when compared to tetrahydrofuran.

In agreement with the paragraphs above, the excited state behavior of arylboron compounds can be attributed to two effects: (a) the influence of the boron atom and (b) extension of π-orbital interactions. The contribution of these two effects to the development of the fluorescence emission is manifested

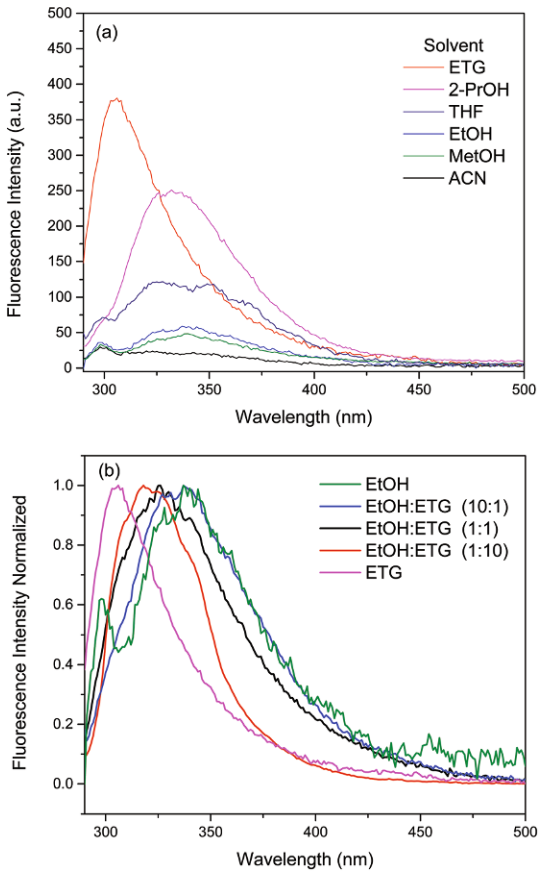

Fig. 2 (a) Fluorescence spectra of $B(Ph)_4^-$ recorded in solvents of different dielectric constant; (b) normalized fluorescence spectra recorded in different viscosity media.

by the significant dipole moment of the B–Ar (trigonal structure) or Ar–B–Ar (tetrahedral structure) moieties, favoring the deactivation of the excited CT-state *via* a non-radiative process by solvent interaction.

The $B(Ph)_3$ structure has an empty p_z-boron atom orbital and π-aryl orbital isolated in the ground state. However, the trigonal excited state shows an extended electronic system, with a rigid structure between the boron atom and just one aryl group. This is observed in the electron orbital contour between the HOMO and LUMO (see scheme in the next section). In fact, the high fluorescence quantum yield for $B(Ph)_3$ is likely to be due to this rigid structure of the B–Ar group in the trigonal structure. DFT calculations (Table S1, ESI†) for the tetrahedral boron species indicate that the arylboron fragment is not planar, unlike in trigonal arylboron compounds, and consequently the fluorescence quantum yield is low for tetraarylborates.

The fluorescence spectrum of tetraphenylborate shows a noticable blue-shift and high values of Φ_F when the solvent viscosity is increased (Fig. 2). This behavior is due to the LE character of the lowest excited state, whereas the TICT state (a CT state with twist motion of the aryl ligand) becomes forbidden because of the high energy necessary for the free rotation of the B–Ar bond. On other hand, the high polarity of

Table 1 Fluorescence quantum yields and maximum emission wavelengths for the arylboron compounds investigated in different solvents

Solvent properties				Triphenylborane		Tetraphenylborate		Tetra(*p*-toluyl)borate	
Solvent	D	ε	η (cP)	$\lambda_{F\ max}$ (nm)	Φ_F	$\lambda_{F\ max}$ (nm)	Φ_F	$\lambda_{F\ max}$ (nm)	Φ_F
ETG	1.69	37.0	16.1	310	0.36	305	0.30	324; 420	0.16
THF	1.75	7.58	0.48	311	0.06	324	0.08	325	0.03
2-PrOH	1.66	17.9	2.30	310	0.30	332	0.08	324; 405	0.03
EtOH	1.69	24.5	1.20	320	0.30	337	0.03	324; 405	0.06
MetOH	1.70	32.7	0.60	322	0.27	338	0.02	324; Und	0.03
ACN	3.47	37.5	0.37	327	0.35	341	0.02	323; Und	0.02

Und = undefined values. D = Dipole moment; ε = dielectric constant. Naphthalene was used as standard for fluorescence emission quantum yield (Φ_F = 0.21);[59] λ_{exc} = 274 nm.

the solvent contributes to the TICT state, promoting electronic extension of the π-orbital in the excited state, with a red shift of the fluorescence maximum emission and low values of Φ_F, as shown in Table 1 for acetonitrile solvent.

The methyl groups in B(*p*-toluyl)$_4^-$ are more efficient electron σ donors, leading to more efficient charge separation. As a result, the fluorescence spectra of B(*p*-toluyl)$_4^-$ (Fig. 3) show two independent emission bands centered at 324 nm and 405 nm, which are assigned to the LE → S_0 and TICT → S_0 transitions, respectively. When both the polarity and viscosity of the solvent is changed to high values (*e.g.* ethylene glycol), the fluorescence spectra of the B(*p*-toluyl)$_4^-$ shows its lowest energetic emission band at 420 nm while the higher energetic emission band is also observed without changes in the maximum fluorescence emission, providing a strong evidence of a non-polarized LE-state.

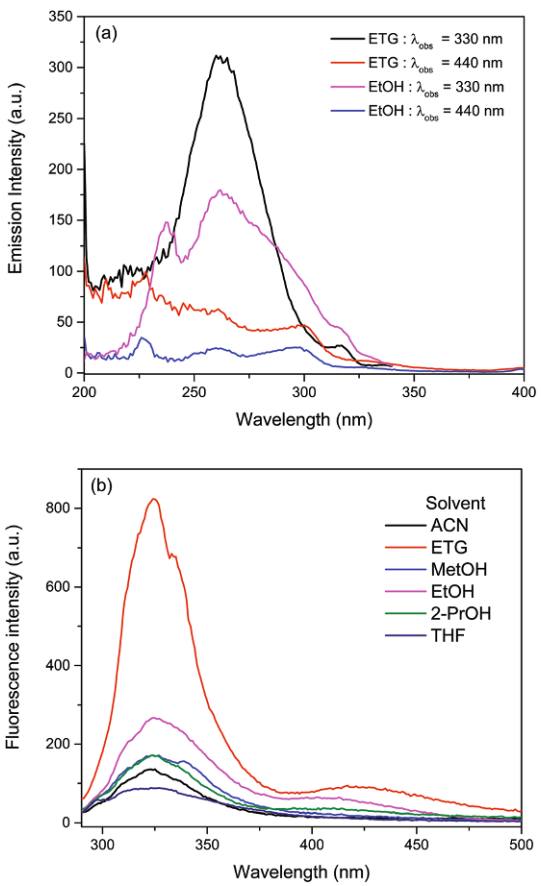

Fig. 3 (a) Excitation spectra of B(*p*-toluyl)$_4^-$ recorded in ethanol and ETG; (b) fluorescence spectra of B(*p*-toluyl)$_4^-$ recorded in solvents of different polarity.

The excitation spectra clearly differ when the fluorescence emission is probed at λ_{obs1} = 330 nm or λ_{obs2} = 440 m (Fig. 3a). The observed low contribution from the band centered at 260 nm for the emission band at λ_{obs2} = 440 nm indicates two different excited states. In fact, time resolved fluorescence measurements performed in ethanol shows a fast and predominant decay component (<1 ps), with an additional longer component decay (Table 2).

The fluorescence quantum yield of the tetrahedral molecule is low in acetonitrile, contrary to that observed for trigonal boron compounds. The high polarity of ACN contributes to the predominance of the CT band, but the absence of the higher energetic band in the fluorescence spectrum of B(*p*-toluyl)$_4^-$ was surprising. The absence of this CT band in more polar solvents (*i.e.* acetonitrile) was previously studied by Angel and co-workers[62] where the effect of polarity of the solvent was

Table 2 Spectroscopic data for arylboron derivatives in ethanol

	Arylboron compounds		
Properties	B(Ph)$_3$	B(Ph)$_4^-$	B(*p*-toluyl)$_4^-$
E_{S1} (eV)	4.16[c,d]; 4.82[e]	4.12[c,d]; 4.60[e]	4.12[c]; 406[d]; 4.48[e]
E_{T1} (eV)	3.45[c]; 3.56[e]	3.58[c]; 3.22[e]	3.54[c]; 3.15[e]
λ_F (nm)	300	337	324; 405
Φ_F (298 K)[b]	0.30	0.03	0.06
τ_F (298 K)	3.93 ns	1.07 ns[a]	2.24 ns[a]
Φ_P (77 K)[b]	0.12	0.02	0.05
τ_P (77 K)	100 ms	2.23 s	1.85 s
λ_T (nm)	350; 370[f]	350; 410[f]	370; 450[f]
τ_T (μs)	1.2; 13.5[f]	0.9; 4.3[f]	2.7; 3.4[f]
$\lambda_{Radical}$ (nm)	300; 325[f]	300; 360[f]	310; 420[f]
$\tau_{Radical}$	>1 ms	>1 ms	>200 μs

[a] Lifetime value for the slowest component decay. The fast component is predominant and undefined (τ_i < 1 ps). [b] Naphthalene was used as fluorescence and phosphorescence standard for quantum yield measurements. [c] Energy values for the monomer. [d] Energy values for the aggregate. [e] Energy values as obtained by DFT calculation. [f] Experimental values measured in acetonitrile.

found to be responsible for the fast deactivation of the excited rhodamine 6G molecule. The absorption behavior in acetonitrile is due to non-radiative deactivation of the CT band by a specific π-donor interaction between the nitrile group (solvent) and the arylboron species.

The charge transfer process in the tetraarylborate anion is completely different from that in the trigonal structure. The higher electronegativity of the boron atom than the phenyl group in the singlet excited state helps us to understand this CT state, where the electron density on the π-bond will reside more toward the boron atom, producing a partial positive charge on Ar and a partial negative charge on boron. This rich electron density on the boron atom will induce a partial negative charge in the other phenyl group, promoting the charge transfer process between one electron-poor phenyl group and one electron-rich phenyl group. This hypothesis is supported by our results with ultrafast absorption spectroscopy and DFT calculations (see Table S2 for the electron density populations, ESI†). These results will be discussed further in a later section.

The CT state is also observed in aggregates[63–65] where the small distance between molecules favors the population of CT states as gateways for direct charge generation. Indeed, we found evidence for aggregation with increasing concentration of the arylboron compounds. The excitation spectrum of the arylboron compounds exhibit a red-shifted band in high concentration media, as observed in Fig. 1. According to exciton theory, the presence of a bathochromic shift associated with this band suggests the formation of J-aggregates.[61,66–70] Fig. 4 shows the red shift of the excitation band of the monomer and aggregate spectra. Evidence for aggregates is also supported by an increase in light scattering with increasing concentration (see Fig. S2, ESI†).[71–73]

The values of the phosphorescence quantum yields at 77 K are shown in Table 2. For tetraarylborate, the phosphorescence yield is lower than that observed for $B(Ph)_3$. However, a long lifetime for phosphorescence was observed for tetraarylborate, suggesting marked differences in structure and photochemical behavior in the triplet states of trigonal *vs.* tetrahedral molecular structures.

Fig. S3 (ESI†) shows the fluorescence and phosphorescence emission of each boron compound at 77 K and room temperature. As expected for the triphenylborane system in ethanol, no difference in the maximum fluorescence intensity was observed at either temperature (Fig. S3a, ESI†). However, at room temperature the tetraarylborate has a red shift (Fig. S3b and S3c, ESI†). This difference in the fluorescence maximum emission is attributed to the high viscosity of ethanol at 77 K, which may indicate that CT-state is generated after LE-deactivation. A detailed explanation about LE and CT-state dependence will be discussed in the ultrafast transient section.

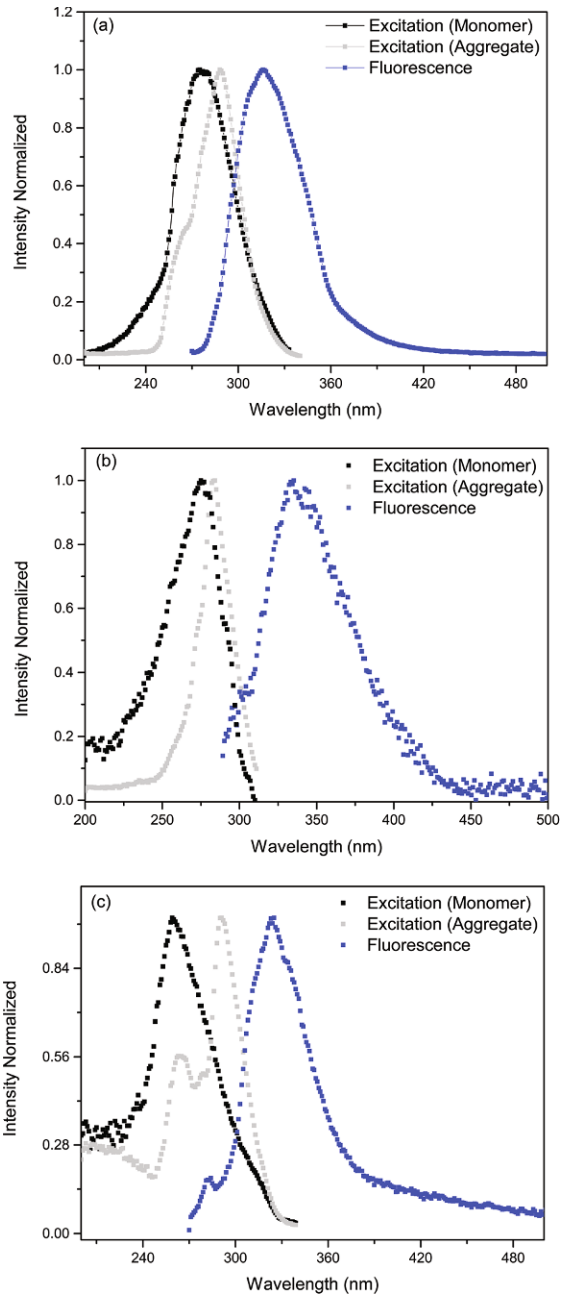

Fig. 4 Excitation and fluorescence emission spectra for the monomer and aggregate of (a) $B(Ph)_3$, (b) $B(Ph)_4^-$, (c) $B(p\text{-toluyl})_4^-$ in ethanol at 298 K.

Theoretical results

DFT calculations were carried out in order to evaluate the singlet and triplet excited state energies and their molecular structures. The B3LYP/6-31+G(d,p) theory level was used in the absence of solvent interaction to illustrate the ground state optimized geometry structures of the trigonal and tetrahedral arylboron compounds, with their molecular orbital contour plots (Table S1 (ESI†) and Scheme 2).

The good agreement between the experimental and calculated energies of the excited singlet and triplet states (see Table 2) indicate that a reasonable approximation for the structures and the orbital densities was achieved.

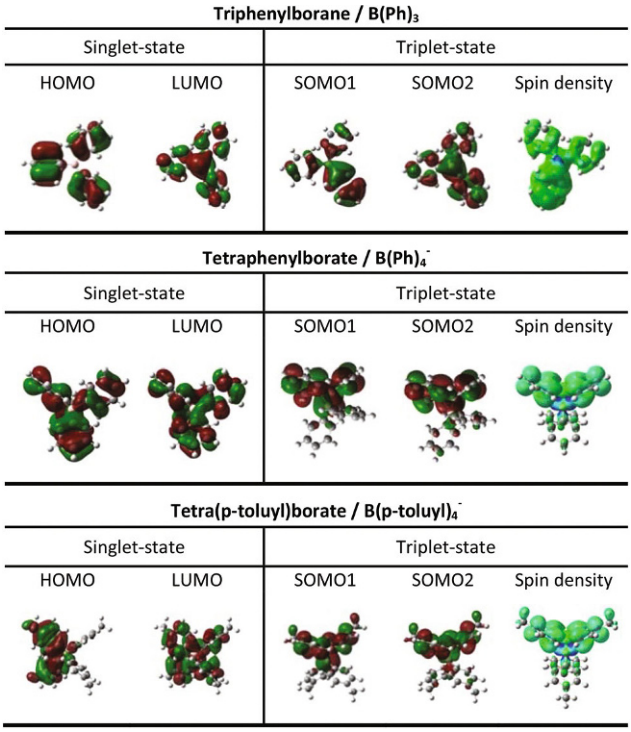

Scheme 2 HOMO, LUMO, SOMO1 and SOMO2 orbital contour plots and electron spin density plots as obtained by DFT calculation. Spin density: the preferred location of the unpaired electron is shown in blue color.

In the trigonal triphenylboron compound, the co-planar configuration of the aromatic rings contributes to the delocalization of the electrons between the aromatic π-orbitals and the vacant boron p_z orbital. The HOMO and LUMO orbital contour plots show the vacant and occupied p_z orbital of the trigonal molecule, respectively. This trigonal boron species does not follow the octet rule, and strong Lewis acid character is expected for the boron atom in the ground state.

In the tetrahedral structure of tetraarylborates, one of the four aryl rings contributes an additional two electrons to populate the boron p_z orbital. As a consequence, the boron atom has a partial negative charge, and the conjugated π-electrons are shifted slightly toward the phenyl groups. However, the nucleophilicity of the boron atom is increased in the excited state, as supported in studies by Bredas and coworkers on the NLO properties of tetraarylborates by the negative values of Re(γ) observed in the excited state.[9]

The LUMO of the tetraarylborate structure shows that two of its phenyl groups are more populated with electron density than the other two groups (see Table S2, ESI†), suggesting that there will be a high polarization of phenyl groups in the excited-state.

Table S2 (ESI†) contains the percentage population obtained by DFT for different fragments of the molecules in the singlet and triplet states. For the BPh3 molecule, the singlet excited state shows an appreciable difference in the population between HOMO and LUMO orbitals, where the empty p_z orbital of the boron atom in the ground state becomes populated in the first singlet excited state (or LUMO).

In the triplet state, the phenyl group and boron atom fragments of the triphenylborane molecule have high electron densities compared to the ground state. Additionally, the populated p_z orbital of boron in the excited-state leads to a triplet state with a significant reduction of electron density in the phenyl ring, indicating an unpaired electron centered on boron atom and the other unpaired electron centered in the phenyl group, as shown in Scheme 2 (blue color). For tetraphenylborate, spin density distributions show that the unpaired electrons are localized between the boron atom and two phenyl groups, (spin density contour in blue color in Scheme 2).

In the HOMO, the orbital population into the four phenyl groups in the tetrahedral molecule is asymmetric, with two of the phenyl groups more populated than the other two. In contrast, in the LUMO, all of the fragments have equal populations. This result provides the first computational evidence for the existence of charge transfer character between the ground state and excited state.

In the triplet state, the optimized structures of the tetrahedral compounds suggest the formation of a bond between two α-carbon atoms on adjacent phenyl-rings. From the DFT calculations, the percentage of orbital population in the triplet state indicates two highly populated fragments, characterized as "biphenyl-like" and the central boron atom (Table S2, ESI†). The deactivation of the triplet state by formation of two phenyl radicals, or formation of a biphenyl fragment, provides strong reasoning for the observation of phenyl and biphenyl photoproducts found in previous work from other laboratories.[5,6,25,33,34,74]

Ultrafast pump–probe femtosecond transient absorption and nanosecond laser flash photolysis

In an effort to directly detect the early stages of excited state formation of these three compounds, their transient absorption spectra and associated decay kinetics were monitored through femtosecond pump–probe experiments in acetonitrile, ethanol and hexanol solutions. The low solubility of all organoboron compounds in solvent of low dielectric solvent rendered studies in THF unfeasible. All solutions were prepared with similar absorbance values (A = 1.7) at the same laser excitation wavelength and all measurements were carried out at room temperature. Samples were excited with 260 nm pump light, which lies within their lowest energy absorption bands, and promotes the population of the S_n excited state; the analysing light was probed in the 340–750 nm range, and the transient absorption spectra evolution and decay kinetics were recorded within a 7 ns time-window. Fig. 5 shows 3D spectra (time, wavelength, and absorption) and kinetic curves for both $B(ph)_4^-$ and $B(p\text{-toluyl})_4^-$.

Comparing the transient absorption spectra of both tetraarylborates (Fig. 5a and b), a strong absorption band is observed at 560 nm. For tetra(p-toluyl)borate, a weak absorption band is

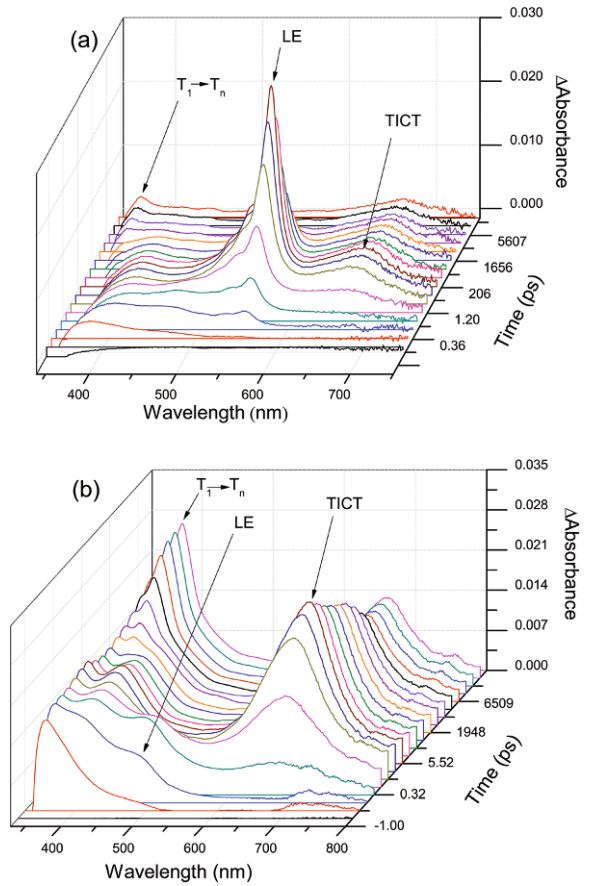

Fig. 5 Ultrafast 3D femtosecond transient absorption spectrum of (a) tetraphenylborate and (b) tetra(*p*-toluyl)borate observed in the 340–800 nm region and collected in the 1 ps–7.5 ns time window. LE = located excited state; TICT = twisted intramolecular charge transfer state.

observed at 480 nm with similar lifetime decay and lifetime growth observed for the tetraphenylborate band at 560 nm. These two absorption bands are assigned to the same transition process (LE → S_n), as supported by the similar energy gap between S_1 (LUMO) and S_2 (LUMO+1) obtained by our DFT calculations. In agreement with previous work on *p*-biphenylyldiazomethane (BDM), an intense band at 490 nm is also attributed to the excited singlet-state (*BDM). The absorption bands around 400–450 nm are observed in both sets of tetraarylborate spectra. However, no assignments were made for these transitions.

The lifetime for the decay of the transient species around 480 nm or 560 nm (LE → S_n transition) has the same time constant as the growth observed for the absorption band around 650–700 nm. In this sense, this last band was attributed to the TICT transition because of the blue-shift observed in the maximum absorption band in acetonitrile solvent, when compared to hexanol or ethanol solvents. Additionally, the absorption band at 560 nm is strongly quenched in acetonitrile, as shown in the Fig. S4 (ESI†). The band at 560 nm grows in times over 5.24 ± 0.41 ps, followed by a decay of 1.06 ± 0.01 ns. The band at 670 nm decay in times over 4.35 ± 0.43 ns, leading to a long-lived residual transient absorption with maximum absorption at 363 nm and τ growth of 6.08 ± 0.04 ns (see Fig. 6a and b).

A closer look at the transient absorption at 363 nm reveals mono-exponential growth kinetics, which were attributed to the triplet state formation. This assignment is confirmed unambiguously by comparison with the absorption band obtained by conventional nanosecond laser flash photolysis (Fig. S5, ESI†).

By nanosecond laser flash photolysis measurements, the absorption (T–T) band of tetraarylborate were recorded in solvents of different polarity. The T–T band maximum is red shifted, with $\Delta\lambda$ = 60 nm and 80 nm for tetraphenylborate and tetra(*p*-toluyl)borate, respectively. For triphenylborane, the red-shift observed in the T–T band was 20 nm. These LFP experiments in solvents of different polarity suggest that the triplet states of tetraarylborates are more polarized than for trigonal molecules.

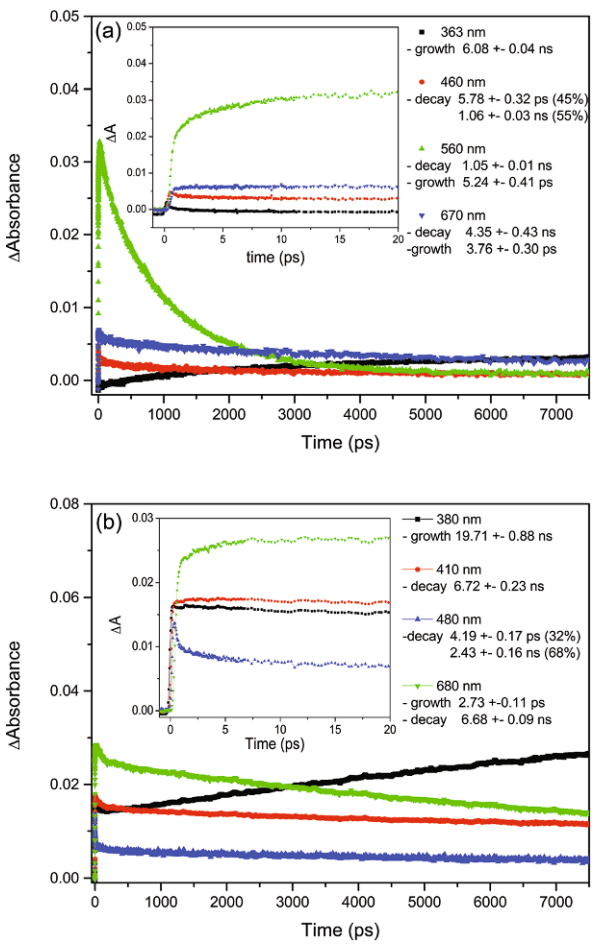

Fig. 6 Ultrafast kinetic time-traces of (a) $B(Ph)_4^-$ and (b) $B(p\text{-toluyl})_4^-$ observed in the 0–7.5 ns time window. Insert displays the kinetic time interval of 1 ps–20 ps.

The influence of solvent polarity on these states can be understood in terms of Coulombic and dispersive interactions between the charge distribution in the solute and the polarizability of the solvent.

The triplet state of arylboron compounds is like a 3π–π^* with CT-character. In highly polar media (*e.g.*, acetonitrile), the triplet-state is stabilized in low values of energy level. However, when the polarity of solvent is lowered (*e.g.*, ethanol), the energy of the triplet state is stabilized due to low CT-character. Consequently, the triplet state energy is increased for solvents with low values of the dielectric constant.

The absence of absorption bands for triphenylborane was also observed for other related structures: 2-aminoethyldiphenyl borane, dimesitylboronic acid, phenylboronic acid and tetra-phenylboroxane (data not shown). This may indicate that both geometry and charge delocalization between two the aryl groups play important roles in determining the photophysical properties of arylboron compounds.

The charge transfer process between two phenyl groups is also observed for the biphenyl molecule, showing the same band around 600–700 nm and attributed to the charge separation or electron transfer process between two polarized groups.[37,75–77] Scheme 3 shows the excited states of tetraarylbroates with rate constants and Fig. S6 (ESI†) shows the 3D absorption spectra of the biphenyl molecule, tetraphenylborate and tetra(*p*-toluyl)borate anions.

Electronic paramagnetic resonance measurements

EPR measurements of all arylboron compounds were carried out at 77 K, following photolysis at 266 nm using a Nd:YAG laser pulses with 20 ns and 3 mJ cm^{-2}, to evaluate the *in situ* radical formation from the excited states of the boron compounds. Fig. 7S (ESI†) shows the radical signal observed at 77 K after irradiation at 266 nm. No further analysis was done to simulate this broad signal, because of the complex hyperfine coupling interactions and anisotropies between the boron atoms and H-atoms in the arylboron structures.

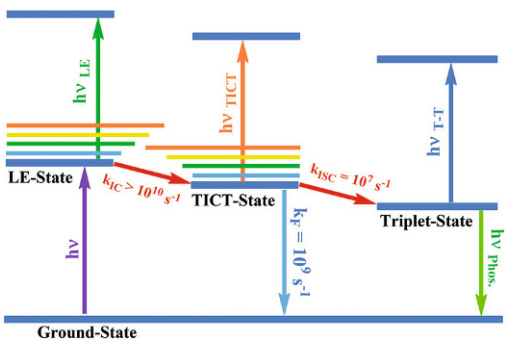

Scheme 3 Jablonski diagram showing the relevant radiative photophysical processes and rate constants where known: absorption ($h\nu$), fluorescence (F) and phosphorescence (P) and non-radiative photophysical processes internal conversion (IC) and intersystem crossing (ISC).

Spin trapping studies. After irradiation of a 10^{-3} mol L^{-1} solution of arylboron compound in the presence of 10^{-2} mol L^{-1} of the spin trap 5,5-dimethyl-1-pyrroline *N*-oxide (DMPO) in oxygen-free solution and at 298 K, a new paramagnetic adduct with lifetime greater than 20 min was observed. No EPR signal was identified when only DMPO was irradiated under same conditions, or when only arylboron compounds were irradiated (at this temperature) in the absence of DMPO, or when the DMPO/boron compound was kept in the dark. Fig. 7 shows the EPR spectra of the $B(Ph)_4^-$/DMPO spin-trapping reaction recorded at 298 K for different irradiation times.

For triphenylborane and tetra(*p*-toluyl)borate, the Ph-DMPO$^\bullet$ radical adduct was observed following 266 nm light irradiation.

The phenyl radical trapped by DMPO shows similar spectra profile and coupling constants previously reported by Buettner[78] a_N = 13.8, a_H = 19.2 in benzene and a_N = 15.8, a_H = 24.4 in aqueous media (pH = 7.0).

In the presence of molecular oxygen, two distinct paramagnetic species are observed in all spectra of trigonal and tetrahedral boron compounds (Fig. 8 and 9).

These radical species are assigned to two different adducts, $(aryl)_2BO$-DMPO$^\bullet$ and (aryl)O-DMPO$^\bullet$, and present similar values of coupling constant to the arylO-DMPO$^\bullet$ radical species previously reported in the literature.[79–81]

The arylO-DMPO$^\bullet$ radical adduct is observed in the spectra of $B(Ph)_3$/DMPO system after irradiation, indicating a B–Ar bond cleavage to yield a phenyl radical and a diphenylboryl radical. For the tetrahedral species, cleavage of two phenyl groups is expected from the excited state, as reported by others.[41,53–55,57–59]

In the presence of the spin trap PBN and oxygen free media, all arylboron compounds yield only one-adduct radical that increase with time of light irradiation. The same coupling

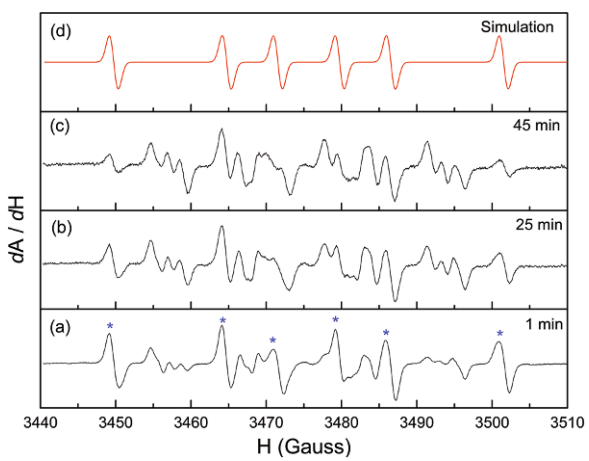

Fig. 7 EPR spectra record at varying irradiation time (a) 1 min, (b) 25 min, and (c) 45 min of a $B(Ph)_4^-$ acetonitrile solution in the presence of DMPO and absence of oxygen molecule. (d) Is the simulated spectra of the Ph-DMPO$^\bullet$ radical adduct. The symbol (*) indicates the spectral lines assigned for the Ph-DMPO$^\bullet$ radical adduct using a_N = 15.00 a_H = 21.80.

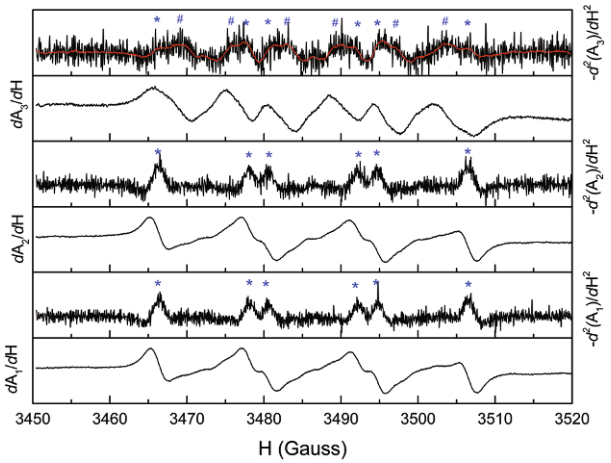

Fig. 8 EPR spectrum of the photoproduct adduct of the tetra(*p*-toluyl) borate (dA_1/dH), tetraphenylborate (dA_2/dH), and triphenylborane (dA_3/dH) in the presence of spin-trap (DMPO) and oxygen (O_2). The second derivative curve is shown by (–d(dA_x)/dH) designation in the EPR spectra. The symbol (*, #) indicate the two independent radical adducts with coupling constant of (*) a_N = 13.90, $a_{H\alpha}$ = 11.70, $a_{H\gamma}$ = 1.20 and (#) a_N = 13.50, $a_{H\alpha}$ = 8.30, a_{B11} = 0.90, a_{B10} = 1.30. The red line shows the smooth curve obtained using the adjacent-averaging method.

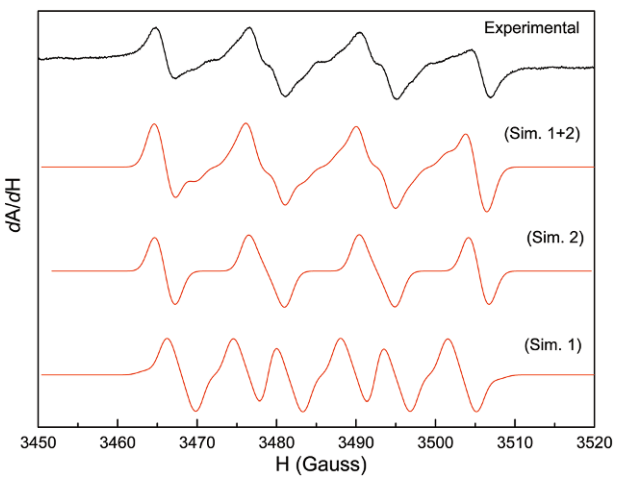

Fig. 9 EPR spectra of the radical adducts from DMPO/B(Ph)$_4^-$ system (Experimental). The Sim 1 + 2 spectrum is the simulated spectra between two independent radical species. The Sim1 and Sim2 curves were simulated with the same coupling constants values from Fig. 3, using signal intensity of 0.24 for Sim1 (#) and 0.76 for Sim 2 (*).

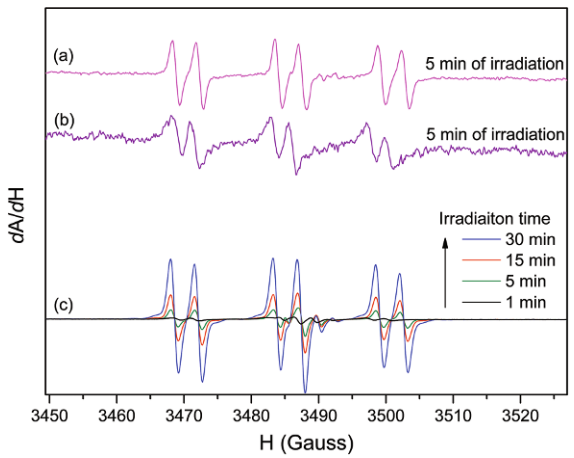

Fig. 10 EPR spectra of the radical adduct between PBN and (a) B(Ph)$_3$, and between PBN and (b) B(*p*-toluyl)$_4^-$, after 5 min of irradiation. (c) EPR spectra of the adduct radical between PBN and B(Ph)$_4^-$ at different times of irradiation.

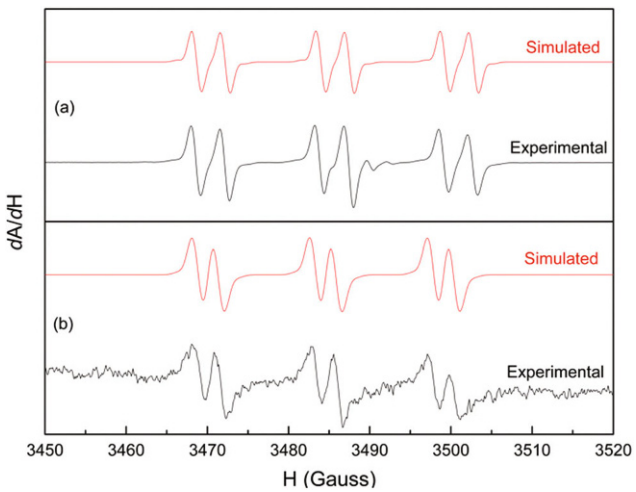

Fig. 11 EPR spectra of arylboron compound-PBN radical adducts, using (top) B(Ph)$_4^-$ and (bottom) B(*p*-toluyl)$_4^-$ after 30 and 5 min of irradiation in free-oxygen media, respectively. The spectra in red (top) shows the simulated curves for the radical adduct of the PBN/B(Ph)$_4^-$ system with a_N = 15.30, a_H = 3.50, a_{B11} = 0.20 and a_{B10} = 0.70; and for the radical adduct of PBN/B(*p*-toluyl)$_4^-$ system with a_N = 14.50, a_H = 2.50, a_{B11} = 0.16 and a_{B10} = 0.80.

constant was found for all adduct radicals of aryl-PBN$^\bullet$ and present similar coupling constant values for the radical adduct Ph-PBN$^\bullet$ previously reported in literature.[78] The experimental and simulation curves are shown in Fig. 10 and 11.

The presence of the arylO-DMPO$^\bullet$ radical adduct in the spectra of the B(Ph)$_3$/DMPO system indicates a reaction between an aryl radical and an oxygen molecule.

For the tetrahedral species, two bond cleavage reactions are expected to yield two phenyl groups or a biphenyl molecule, as expected from the triplet excited state deactivation. Schemes 4 and 5 summarizes the proposed mechanism for photoreaction of excited-states of tetrahedral and trigonal-boron compounds in the presence of the spin-trapping molecules (PBN and DMPO).

In the literature of boron compound photochemistry, several authors have reported phenyl radicals and boroxyl radicals as products of photolysis, for example the effect of oxidizing agents that can generate other products.[26–34] However, the use of spin traps was not properly performed to elucidate the first radicals generated after photolysis of trigonal and tetrahedral boron compounds.

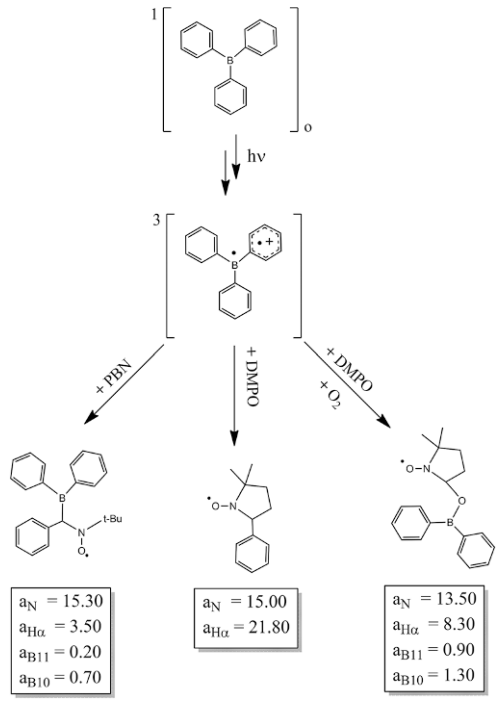

Scheme 4 Predominant radical detected by EPR-experiments after irradiation of trigonal-boron compound and subsequent chemical reaction with spin trap (DMPO or PBN).

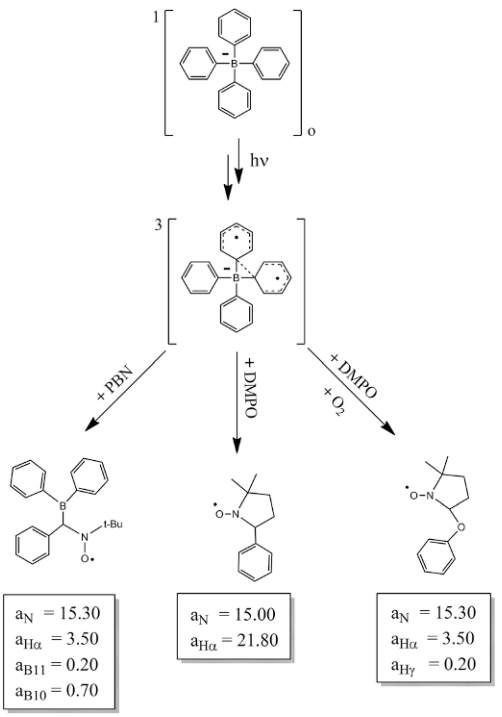

Scheme 5 Predominant radical detected by EPR-experiments after irradiation of tetrahedral-boron compound and subsequent chemical reaction with spin trap (DMPO or PBN).

Conclusions

The excited state reactivity and photophysical characterization of triphenylborane, tetraphenylborate and tetra(*p*-toluyl)borate have been studied through ultrafast pump–probe femtosecond transient absorption, nanosecond laser flash photolysis, spin trapping studies with EPR spectroscopy, and DFT calculations. Our results provide a relatively complete description of the excited state deactivation pathways of arylboron compounds. For the tetrahedral compounds, it is suggested that a TICT state results from a charge transfer process between two of the phenyl groups. The lack of a TICT transition in the trigonal molecules is attributed to the rigid structure between the boron atom and the phenyl groups, that does not allow changes in the symmetry of the π-orbitals, and consequently, the absence of a twist motion in the excited-state. Pump–probe experiments with the tetra(*p*-toluyl)borate derivative have revealed that, due to the electron inductive effect of the methyl groups, the LE state is quickly deactivated to the TICT state. Femtosecond pump–probe experiments confirm the extension of the π-orbital between two aryl groups in tetraaryborates, as has previously been observed for the biphenyl molecule.

The T–T band is red shifted in solvents of high polarity, indicating the presence of significant CT character in the triplet state of the arylboron compounds. The triplet state is the precursor for B–Ar bond cleavage to yield aryl diphenylboryl radicals. In the presence of oxygen, aryloxyl and diphenylboryloxyl species are also observed through the EPR signals of the trapped radicals.

Acknowledgements

The authors acknowledge FAPESP (Grants 2015/13756-1, 2012/19823-4, 2011/51555-7 and 2009/54040-8), and the Coimbra Chemistry Centre through the Fundação para a Ciência e a Tecnologia (FCT Project UID/QUI/UI0313/2013) and COMPETE for financial support. MDEF thanks the National Science Foundation for continued support of his research program through grant CHE-1464817.

Notes and references

1 K. Imakita, M. Ito, R. Naruiwa, M. Fujii and S. Hayashi, Enhancement of ultrafast nonlinear optical response of silicon nanocrystals by boron-doping, *Opt. Lett.*, 2012, **37**, 1877.

2 P. Kumbhakar, A. K. Kole, C. S. Tiwary, S. Biswas, S. Vinod, J. Taha-Tijerina, U. Chatterjee and P. M. Ajayan, Nonlinear Optical Properties and Temperature-Dependent UV-Vis Absorption and Photoluminescence Emission in 2D Hexagonal Boron Nitride Nanosheets, *Adv. Opt. Mater.*, 2015, 828–835.

3 R. J. Shiue, Y. Gao, Y. Wang, C. Peng, A. D. Robertson, D. K. Efetov, S. Assefa, F. H. L. Koppens, J. Hone and

D. Englund, Responsivity Graphene-Boron Nitride Photodetector and Autocorrelator in a Silicon Photonic Integrated Circuit, *Nano Lett.*, 2015, **15**, 7288–7293.
4 S. Mukherjee and P. Thilagar, Boron clusters in luminescent materials, *Chem. Commun.*, 2016, **52**, 1070–1093.
5 C. D. Entwistle and T. B. Marder, Boron Chemistry Light the Way: Optical Properties of Molecular and Polymeric Systems, *Angew. Chem., Int. Ed.*, 2002, **41**, 2927–2931.
6 C. D. Entwistle and T. B. Marder, Applications of three-coordinate organoboron compounds and polymers in optoelectronics, *Chem. Mater.*, 2004, **16**, 4574–4585.
7 S. Yamaguchi and A. Wakamiya, Boron as a key component for new π-electron materials, *Pure Appl. Chem.*, 2006, **78**, 1413–1424.
8 F.-W. Gao, R.-L. Zhong, S.-L. Sun, H.-L. Xu, L. Zhao and Z.-M. Su, Charge transfer and first hyperpolarizability: cage-like radicals C59X and lithium encapsulated Li@C59X (X=B, N), *J. Mol. Model.*, 2015, **21**, 258.
9 R. L. Gieseking, T. R. Ensley, H. Hu, D. J. Hagan, C. Risko, E. W. Van Stryand and J.-L. Bredas, Nonlinear Optical Properties of X(C6H5)(4) (X=B-, C, N+, P+): A New Class of Molecules with a Negative Third-Order Polarizability, *J. Am. Chem. Soc.*, 2015, **137**, 9635–9642.
10 S. Muhammad, H. Xu, Z. Su, K. Fukuda, R. Kishi, Y. Shigeta and M. Nakano, A new type of organic–inorganic hybrid NLO-phore with large off-diagonal first hyperpolarizability tensors: a two-dimensional approach, *Dalton Trans.*, 2013, **42**, 15053.
11 Z. Q. Liu, Q. Fang, D. X. Cao, D. Wang and G. B. Xu, Triaryl boron-based A-π-A vs triaryl nitrogen-based D-π-D quadrupolar compounds for single- and two-photon excited fluorescence, *Org. Lett.*, 2004, **6**, 2933–2936.
12 A. Sundararaman, K. Venkatasubbaiah, M. Victor, L. N. Zakharov, A. L. Rheingold and F. Jakle, Electronic communication and negative binding cooperativity in diborylated bithiophenes, *J. Am. Chem. Soc.*, 2006, **128**, 16554–16565.
13 J. Hockemeyer, A. Castel, P. Rivi and W. J. Blau, Synthesis and Optical Properties of Group 14 Element – Thienyl Polymers, *Appl. Organomet. Chem.*, 1997, **11**, 513–521.
14 J. C. Calabrese and W. Tam, Organometallics for non-linear optics: Metal-pyridine and bipyridine complexes, *Chem. Phys. Lett.*, 1987, **133**, 244–245.
15 P. G. Pickup, Conjugated metallopolymers. Redox polymers with interacting metal based redox sites, *J. Mater. Chem.*, 1999, **9**, 1641–1653.
16 N. Hari Singh, Organometallic materials for nonlinear optics, *Appl. Organomet. Chem.*, 1991, **5**, 349–377.
17 R. Zhang, J. Fan, X. Zhang, H. Yu, H. Zhang, Y. Mai, T. Xu, J. Wang and H. J. Snaith, Nonlinear Optical Response of Organic-Inorganic Halide Perovskites, *ACS Photonics*, 2016, **3**, 371–377.
18 E. Cariati, M. Pizzotti, D. Roberto, F. Tessore and R. Ugo, Coordination and organometallic compounds and inorganic-organic hybrid crystalline materials for second-order non-linear optics, *Coord. Chem. Rev.*, 2006, **250**, 1210–1233.
19 B. S. Kalanoor, L. Gouda, R. Gottesman, S. Tirosh, E. Haltzi, A. Zaban and Y. R. Tischler, Third order optical nonlinearities in organometallic methylammonium lead iodide perovskite thin films, *ACS Photonics*, 2016, **3**, 361–370.
20 P. Sakthi, R. Rajasekaran and D. Balasubramanian, Growth, Optical, Thermal and Mechanical Behavior of an Organometallic Nonlinear Optical-Thiocyanate Thiourea Potassium Chloride Crystal, *J. Adv. Phys.*, 2016, **5**, 199–206.
21 A. Cesaretti, B. Carlotti, G. Consiglio, T. Del Giacco, A. Spalletti and F. Elisei, Inclusion of two push–pull N-methylpyridinium salts in anionic surfactant solutions: A comprehensive photophysical investigation, *J. Phys. Chem. B*, 2015, **119**, 6658–6667.
22 C. Cui, R. A. Lalancette and F. Jäkle, The elusive tripodal tris(2-pyridyl)borate ligand: a strongly coordinating tetraarylborate, *Chem. Commun.*, 2012, **48**, 6930–6932.
23 S. N. Margar, L. Rhyman, P. Ramasami and N. Sekar, Molecular and Biomolecular Spectroscopy Fluorescent difluoroboron-curcumin analogs: An investigation of the electronic structures and photophysical properties, *Spectrochim. Acta, Part A*, 2016, **152**, 241–251.
24 Y. Kubota, Y. Sakuma, K. Funabiki and M. Matsui, Solvatochromic fluorescence properties of pyrazine-boron complex bearing a β-iminoenolate ligand, *J. Phys. Chem. A*, 2014, **118**, 8717–8729.
25 M. Elbing and G. C. Bazan, A new design strategy for organic optoelectronic materials by lateral boryl substitution, *Angew. Chem.,– Int. Ed.*, 2008, **47**, 834–838.
26 C. L. Crawford, M. R. Gholami, R. N. Bhave and R. J. Hanrahan, Pulse Radiolysis of Aqueous Solutions of Sodium Tetraphenylborate, *Radiat. Phys. Chem.*, 1994, **44**, 309–315.
27 J. C. Doty, P. J. Grisdale, T. R. Evans and J. L. R. Williams, Boron photochemistry .7. Photochemically induced electron transfer from tetraphenylborate anion to singlet oxygen, *J. Organomet. Chem.*, 1971, **32**, 35–37.
28 J. C. Doty, B. Babb, P. J. Grisdale, M. Glogowski and J. L. R. Williams, Donor Acceptor Boron Nitrogen, *J. Organomet. Chem.*, 1972, **38**, 229–236.
29 J. J. Eisch, J. H. Shah and M. P. Boleslawski, Skeletal rearrangements of arylborane complexes mediated by redox reactions: thermal and photochemical oxidation by metal ions, *J. Organomet. Chem.*, 1994, **464**, 11–21.
30 A. Pelter, R. T. Pardasani and P. Pardasani, The Photochemistry of Boron Compounds, *Tetrahedron*, 2000, **56**, 7339–7369.
31 B. G. Ramsey and M. E. Bier, A laser desorption ionization mass spectrometry investigation of triarylboranes and tri-9-anthrylborane photolysis products, *J. Organomet. Chem.*, 2005, **690**, 962–971.
32 G. B. Schuster, X. Yang, C. Zou and B. Sauerwein, Ion pairs: energy, distance and solvent dependence, *J. Photochem. Photobiol., A*, 1992, **65**, 191–196.
33 J. L. R. Williams, J. C. Doty, P. J. Grisdale, R. Searle, T. H. Regan, G. P. Happ and D. P. Maier, Boron Photochemistry. I. Irradiation of Sodium Tetraarylborates

in Aqueous Solution, *J. Am. Chem. Soc.*, 1967, **89**, 5153–5157.
34 J. L. R. Williams, J. C. Doty, P. J. Grisdale, T. H. Regan, G. P. Happ and D. P. Maier, Boron Photochemistry. II. Irradiation of Sodium Tetraarylborate in Alcohol Solutions, *J. Am. Chem. Soc.*, 1968, **90**, 53–55.
35 C. Huang, C. Chen, M. Zhang, L. Lin, X. Ye, S. Lin, M. Antonietti and X. Wang, Carbon-doped BN nanosheets for metal-free photoredox catalysis, *Nat. Commun.*, 2015, **6**, 7698.
36 S.-Y. Kim, A.-R. Lee, Y.-J. Cho, H.-J. Son, W.-S. Han and S. O. Kang, Photochemistry of hybrid organic–inorganic triarylborane-o-carboranes, *J. Organomet. Chem.*, 2015, **798**, 245–251.
37 M. Z. Zgierski, E. C. Lim and T. Fujiwara, Intramolecular Charge Transfer in di-tert-butylaminobenzonitriles and 2,4,6-tricyanoanilines: A Computational TDDFT Study, *Comput. Theor. Chem.*, 2014, **1036**, 1–6.
38 S. Chai and S.-L. Cong, Intermolecular Hydrogen Bond and Twisted Intramolecular Charge Transfer in Excited State of Fast Violet B (FVB) in Methanol Solution, *Spectrochim. Acta, Part A*, 2014, **125**, 67–72.
39 D. Frath, J. E. Yarnell, G. Ulrich, F. N. Castellano and R. Ziessel, Ultrafast photoinduced electron transfer in viologen-linked BODIPY dyes, *ChemPhysChem*, 2013, **14**, 3348–3354.
40 B. Carlotti, E. Benassi, V. Barone, G. Consiglio, F. Elisei, A. Mazzoli and A. Spalletti, Effect of the pi bridge and acceptor on intramolecular charge transfer in push–pull cationic chromophores: An ultrafast spectroscopic and TD-DFT computational study, *ChemPhysChem*, 2015, **16**, 1440–1450.
41 J. De Jonghe-Risse, J. Heier, F. Nueesch and J. E. Moser, Ultrafast Charge Transfer in Cyanine Borate Solid-State Films and Blends with Fullerene, *J. Mater. Chem. A*, 2015, 10935–10941.
42 J. De Jonghe-Risse, J. Heier, F. Nueesch and J. E. Moser, Ultrafast Charge Transfer in Cyanine Borate Solid-State Films and Blends with Fullerene, *J. Mater. Chem. A*, 2015, **3**, 10935–10941.
43 T. Miura, K. Maeda, H. Murai and T. Ikoma, Long-Distance Sequential Charge Separation at Micellar Interface Mediated by Dynamic Charge Transporter: A Magnetic Field Effect Study, *J. Phys. Chem. Lett.*, 2015, **6**, 267–271.
44 J. Wang, G. Burdzinski, T. L. Gustafson and M. S. Platz, Ultrafast study of p-biphenylyldiazomethane and p-biphenylylcarbene, *J. Org. Chem.*, 2006, **71**, 6221–6228.
45 R. Hu, E. Lager, A. Aguilar-Aguilar, J. Liu, J. W. Y. Lam, H. H. Y. Sung, I. D. Williams, Y. Zhong, K. S. Wong, E. Pena-Cabrera and B. Z. Tang, Twisted intramolecular charge transfer and aggregation-induced emission of BODIPY derivatives, *J. Phys. Chem. C*, 2009, **113**, 15845–15853.
46 J. Wang, Y. Wang, T. Taniguchi, S. Yamaguchi and S. Irle, Substituent effects on twisted internal charge transfer excited states of N-borylated carbazoles and (diphenylamino)boranes, *J. Phys. Chem. A*, 2012, **116**, 1151–1158.
47 D. Oesch and N. W. Luedtke, Fluorescent chemosensors of carbohydrate triols exhibiting TICT emissions, *Chem. Commun.*, 2015, **51**, 12641–12644.
48 P. Shen, M. Li, C. Liu, W. Yang, S. Liu and C. Yang, Two Sensitive Fluorescent BOPIM Probes with Tunable TICT Character for Low-Level Water Detection in Organic Solvents, *J. Fluoresc.*, 2016, **26**, 363–369.
49 S. Ozcelik, G. K. Karaoglan, G. Gumrrku, A. Erdogmus and A. Gul, Photophysical and photochemical properties of a zinc phthalocyanine with four diphenylborinic ester moieties, *J. Organomet. Chem.*, 2014, **769**, 17–23.
50 Z. Zhou, A. Wakamiya, T. Kushida and S. Yamaguchi, Planarized triarylboranes: Stabilization by structural constraint and their plane-to-bowl conversion, *J. Am. Chem. Soc.*, 2012, **134**, 4529–4532.
51 M. Schäfer, J. Schäfer, R. D. Dewhurst, W. C. Ewing, M. Krahfuß, M. W. Kuntze-Fechner, M. Wehner, C. Lambert and H. Braunschweig, Regioselective Catalytic and Stepwise Routes to Bulky, Functional-Group-Appended, and Luminescent 1,2-Azaborinines, *Chem. – Eur. J.*, 2016, **22**, 8603–8609.
52 O. V. Antonova, V. A. Nadolinnyi, E. A. Il'inchik, O. P. Yur'eva and A. A. Ryadun, Triplet exciton states in ammonium tetraphenylborate crystals, *Bull. Lebedev Phys. Inst.*, 2009, **36**, 356–358.
53 J. C. S. N. J. Turro and V. Ramamurthy, *Modern Molecular Photochemistry of Organic Molecules*, University Science Books, 2010.
54 J. C. S. N. J. Turro and V. Ramamurthy, *Principles of Molecular Photochemistry: An Introduction*, University Science Books, 2010.
55 C. G. Bochet, *Comprehensive Organic Synthesis*, 2nd edn, 2014, vol. 9, pp. 330–350.
56 H. B. E. Lippert and W. Lüder, in *Advances in Molecular Spectroscopy*, ed. A. Magnini, Pergamon Press, Oxford, 1962.
57 P. J. Grisdale, J. L. R. Willians, M. E. Glogowski and B. E. Babb, Boron Photochemistry. VI. The Possible Role of Bridged Intermediates in the Photolysis of Borate Complexes, *J. Org. Chem.*, 1971, **1**, 544–549.
58 N. Matsumi, M. Miyata and Y. Chujo, Synthesis of organoboron π-conjugated polymers by hydroboration polymerization between heteroaromatic diynes and mesitylborane and their light emitting properties, *Macromolecules*, 1999, **32**, 4467–4469.
59 B. Valeur and M. N. Berberan-Santos, *Molecular Fluorescence: Principles and Applications*, Wiley-VCH, 2nd edn, 2012.
60 T. Alaviuhkola, J. Bobacka, M. Nissinen, K. Rissanen, A. Ivaska and J. Pursiainen, Synthesis, characterization, and complexation of tetraarylborates with aromatic cations and their use in chemical sensors, *Chem. – Eur. J.*, 2005, **11**, 2071–2080.
61 S. Choi, J. Bouffard and Y. Kim, Aggregation-induced emission enhancement of a meso-trifluoromethyl BODIPY via J-aggregation, *Chem. Sci.*, 2014, **5**, 751–755.

62 G. Angel, R. Gagel and A. Laubereau, Fentosecond relaxation dynamics in the electronic ground state of dye molecules studied by polarization-dependent amplification spectroscopy, *Chem. Phys. Lett.*, 1989, **156**, 169–174.

63 S. Verma and H. N. Ghosh, Exciton Energy and Charge Transfer in Porphyrin Aggregate/Semiconductor (TiO2) Composites, *J. Phys. Chem. Lett.*, 2012, **3**, 1877–1884.

64 J. Guasch, L. Grisanti, M. Souto, V. Lloveras, J. Vidal-Gancedo, I. Ratera, A. Painelli, C. Rovira and J. Veciana, Intra- and Inter-Molecular Charge-Transfer in Aggregates of Tetrathiafulvalene -Triphenylmethyl Radical Derivatives in Solution, *J. Am. Chem. Soc.*, 2013, **135**, 1–11.

65 D. Fazzi, M. Barbatti and W. Thiel, Unveiling the Role of Hot Charge-Transfer States in Molecular Aggregates via Nonadiabatic Dynamics, *J. Am. Chem. Soc.*, 2016, **138**, 4502–4511.

66 N. Venkatramaiah, B. Ramakrishna, R. Venkatesan, F. a. A. Paz and J. P. C. Tomé, Facile synthesis of highly stable BF3-induced meso-tetrakis (4-sulfonato phenyl) porphyrin (TPPS4)-J-aggregates: structure, photophysical and electrochemical properties, *New J. Chem.*, 2013, **37**, 3745.

67 L. Yao, F. Dan, W. Liu, Q. Cao, C. Yang, K. Zou and S. Xiao, Solid-state red emission of boron-fluorine complexes with extended π-conjugated structure, *J. Fluorine Chem.*, 2013, **156**, 187–191.

68 T. T. Vu, M. Dvorko, E. Y. Schmidt, J. F. Audibert, P. Retailleau, B. A. Trofimov, R. B. Pansu, G. Clavier and R. Meallet-Renault, Understanding the spectroscopic properties and aggregation process of a new emitting boron dipyrromethene (BODIPY), *J. Phys. Chem. C*, 2013, **117**, 5373–5385.

69 B. V. Bukvetskii, E. V. Fedorenko, A. G. Mirochnik and A. Y. Beloliptsev, Crystal Structure and Luminescence of 2,2-Ddifluoro-4,6-(4-methylphenyl)- 1,3,2-dioxaborine, *J. Struct. Chem.*, 2012, **53**, 73–81.

70 K. Šišková, B. Vlčková and P. Mojzeš, Spectral detection of J-aggregates of cationic porphyrin and investigation of conditions of their formation, *J. Mol. Struct.*, 2005, **744-747**, 265–272.

71 W. G. Santos, T. T. Tominaga, O. R. Nascimento, C. C. Schmitt and M. G. Neumann, Phototransients of 2-ethylaminodiphenylborinate generated by direct photolysis and photosensitization, *J. Photochem. Photobiol., A*, 2012, **236**, 14–20.

72 W. G. Santos, C. C. Schmitt and M. G. Neumann, Photochemistry of tetraphenyldiboroxane and its use as photopolymerization coinitiator, *Photochem. Photobiol.*, 2013, **89**, 1362–1367.

73 W. G. Santos, D. R. Cardoso, L. D. O. R. Arrivetti, C. C. Schmitt and M. G. Neumann, DFT, spectroscopic, and photoproduct study of 2-aminoethyldiphenylborinate and tetraphenyldiboroxane, *J. Organomet. Chem.*, 2014, **755**, 125–133.

74 S. T. Murphy, C. F. Zou, J. B. Miers, R. M. Ballew, D. D. Dlott and G. B. Schuster, Tetraarylborates ([AR]4B-) - estimation of oxidation potentials and reorganization energies from eletron-transfer rates, *J. Phys. Chem.*, 1993, **97**, 13152–13157.

75 W. Verbouwe, L. Viaene, M. Van der Auweraer, F. C. De Schryver, H. Masuhara, R. Pansu and J. Faure, Photoinduced Intramolecular Charge Transfer in Diphenylamino Substituted Triphenylbenzene, Biphenyl and Fluorene, *J. Phys. Chem. A*, 1997, **101**, 8157–8165.

76 J. Benzler and K. Luther, Rotational relaxation of biphenyl and p-terphenyl in n-alkanes: the breakdown of the hydrodynamic description, *Chem. Phys. Lett.*, 1997, **279**, 333–338.

77 P. Song, S.-G. Sun, J.-Y. Liu, Y.-Q. Xu, K.-L. Han and X.-J. Peng, Theoretical and experimental study on the intramolecular charge transfer excited state of the new highly fluorescent terpyridine compound, *Spectrochim. Acta, Part A*, 2009, **74**, 753–757.

78 G. R. Buettner, Spin Trapping - Electron-Spin-Resonance Parameters of Spin Adducts, *Free Radicals Biol. Med.*, 1987, **3**, 259–303.

79 G. L. Mills and L. R. Sullivan, Indirect Photolysis of Tetraphenylborate Sensitized by Humic Acid, *Chemosphere*, 1995, **31**, 4541–4547.

80 J. L. R. Willians, J. C. Doty, P. J. Grisdale, T. H. Regan and D. G. Borde, Boron Photochemistry: 1 -Phenylcyclohexall, 4-diene from Sodium Tetraphenylborate, *J. Org. Chem.*, 1967, 109.

81 W. G. Santos, C. C. Schmitt and M. G. Neumann, Polymerization of HEMA photoinitiated by the Safranine/diphenylborinate system, *J. Photochem. Photobiol., A*, 2013, **252**, 124–130.